Optical detection of electron-nuclear double resonance for an $S=1$ luminescent center in GaP:O

J. F. Donegan,* D. Y. Jeon, and G. D. Watkins
Sherman Fairchild Laboratory 161, Department of Physics, Lehigh University, Bethlehem, Pennsylvania 18015
(Received 20 August 1990)

The origin of a triplet ($S=1$) optically detected magnetic-resonance (ODMR) spectrum observed in the luminescence of GaP:O has been the subject of recent controversy. Originally identified with the negative-charge state of a substitutional oxygen impurity, more recent suggestions have interpreted a resolved $I=\frac{3}{2}$ hyperfine interaction in the ODMR to indicate an interstitial-gallium-related defect. We report here optical detection of electron-nuclear double resonance (ODENDOR) of the central $I=\frac{3}{2}$ nucleus and confirm unambiguously that it is gallium. Its magnetic hyperfine and nuclear quadrupole interactions are determined and an improved analysis of the electron spin Hamiltonian is presented. A possible model for the defect is suggested: a $\langle 100\rangle$-oriented $Ga_i V_{Ga}$ pair stabilized by the presence of one or two nearby substitutional oxygen donors. The ODENDOR spectrum arises from the $M=0$ state, causing unusual magnetic-field and orientation effects. The origin of these effects is described and the procedure of analysis to extract the hyperfine parameters is outlined.

I. INTRODUCTION AND BACKGROUND

As a system, the isolated oxygen donor (O_P) in GaP has received one of the most thorough of spectroscopic studies.[1] Most of the studies have concentrated on two prominent luminescence bands which have been established to be related to the oxygen defect:[2,3] (1) donor-acceptor pair (DA) luminescence at ~ 1.3 eV between O_P^0 and shallow acceptors which serves to locate the oxygen donor level $(0/+)$ at $E_c-0.893$ eV, and (2) an electron capture luminescence at 0.841 eV between an excited and ground state of O_P^0. (A third luminescence band[4] at 0.53 eV and an absorption band[5] at 1.74 eV have also been established to arise from the oxygen defect and have been interpreted to arise from electron-capture luminescence for O_P^- and the corresponding pseudoacceptor bound-excitation absorption at O_P^0, respectively.)

In spite of this detailed study, a microscopic model of the electronic structure of the oxygen defect which is universally accepted has not been found. Two models have been proposed to describe the spectroscopic data. The model of Dean[1] suggests that oxygen is a simple substitutional donor on the P sublattice which possesses a very large central-cell effect. In his model, the 0.841-eV electron-capture luminescence is from the excited $1S(E)$ to the ground $1S(A_1)$, effective-mass states of O_P^0. The alternative model, due to Morgan,[6] is that of a deep unperturbed central O_P^0 core with the ground and excited electronic states coming from the weakly bonding "vacancy" states of the gallium neighbors. In his model, the 0.841-eV electron-capture luminescence is between molecular-orbital "vacancy" states.

Magnetic-resonance studies, usually very effective in extracting microscopic information, have resulted in further controversy. In the original optical detection of magnetic resonance (ODMR) carried out on GaP:O, Gal, Cavenett, and Smith[7] observed in the 0.841-eV luminescence band a triplet ($S=1$) resonance showing a strong resolved hyperfine interaction with a single Ga nucleus. These authors concluded that the ODMR signal was due to the negative (O_P^-) charge state of oxygen challenging the O_P^0 electron-capture luminescence interpretation. A follow-up study by Gal, Cavenett, and Dean[4] using Zeeman and stress measurements led to a reinterpretation of the ODMR results. The ODMR detection mechanism was assigned instead to a spin-dependent Auger process in which the O_P^- center seen by ODMR dissociates with one electron recombining with a hole on an acceptor and the neutral O_P^0 is then left in the $1S(E)$ excited state which subsequently emits the 0.841-eV photon. A further series of studies concerned principally with angular dependence and time evolution of the ODMR resonance was carried out by Dawei and Cavenett.[8] The time-resolved measurements showed that the lifetime measured in ODMR was about a factor of 10 longer than that of the oxygen-related electron-capture luminescence transition. Despite this, Dawei and Cavenett maintained that there was a direct association between oxygen and the ODMR resonance. They noted also that the ODMR signal could be detected in the 1.3-eV DA pair band, further strengthening the connection to the oxygen donor.

More recent ODMR measurements by Lee[9] and Godlewski and Monemar[10] have thrown doubt on this interpretation. Spectral dependence measurements by these authors of the $S=1$ ODMR signal showed a marked disparity between the oxygen-related DA pair luminescence band position and the corresponding luminescence band giving rise to the triplet ODMR. A further reinterpretation was proposed: the triplet ODMR resonance is due to an interstitial-gallium (Ga_i) -related defect and not related to oxygen at all. (The Ga_i identification was bolstered by the work of Lee[9] in which he detected an additional isotropic $S=\frac{1}{2}$ ODMR signal labeled KL1, which he identified as arising from isolated

Ga_i^{2+}.) The hyperfine interaction for this new center was approximately twice that for the $S=1$ center, as expected for a one-particle ($S=\frac{1}{2}$) versus a two-particle ($S=1$) state. The controversy over interpretation arose again in a Comment by Gal[11] and a reply by Godlewski and Monemar.[12] Gal maintained that the new interpretation was not based on sound experimental facts though he did not appear to have been aware of the new center observed by Lee.

In this paper, we report the results of an ODMR and an optical detection of electron-nuclear double resonance (ODENDOR) study of this $S=1$ ODMR signal. We detect directly by ODENDOR the nuclear magnetic resonance of the central nucleus which gives rise to the resolved hyperfine structure in the ODMR and provide the first direct confirmation that is in indeed gallium. (Other possible candidates included chlorine and copper, which also have two major abundant $I=\frac{3}{2}$ isotopes of comparable abundance ratios.) Quadrupole interactions and the components of the magnetic hyperfine tensor for the central gallium nucleus have also been obtained. We interpret our results to be consistent with a Ga_i-related defect but our results provide no direct information concerning the possible incorporation of oxygen in the defect or not. Finally, we suggest a new possible model for the defect as a $\langle 100 \rangle$-oriented Ga_i-V_{Ga} pair, stabilized by the presence of one or two substitutional donors.

An interesting result of our study is the recognition that the ENDOR transitions being observed are occurring in the electronic spin $M=0$ state. In this case, since there are no first-order magnetic hyperfine effects, second- and higher-order effects must be considered. These in turn can serve to produce anomalous apparent nuclear g values and large anisotropies in the ODENDOR spectra which are unrelated to the true anisotropies of the hyperfine interactions. We demonstrate here that with a proper analysis all of the relevant nuclear hyperfine interactions can still be extracted.

Although ODMR has often been applied to $S=1$ excited states via luminescence in semiconductors, there have been few reported ODENDOR studies. Because the $M=0$ state is often the bottleneck state in such systems, we can anticipate that future ODENDOR studies will also find that the transitions being observed arise from this state. The general features that we outline here should therefore be of value for subsequent ODENDOR studies in such systems.

II. EXPERIMENTAL TECHNIQUES

The luminescence, ODMR, and ODENDOR measurements were carried out in an Oxford Instruments SM-4 superconducting magnet optical cryostat providing magnetic fields up to 3 T. The sample was placed in a 35-GHz TE_{011} microwave cavity designed to have optical access.[13] A two-turn coil mounted in the cavity such that its magnetic-field axis is perpendicular to both the static and microwave magnetic fields was used for the ODENDOR experiments. A combination of a Fluke 6060B frequency synthesizer and an ENI 3100 LA amplifier supplied the radio-frequency current to the ODENDOR coil. The luminescence was excited by ~40 mW of the 514.5-nm line of an Ar^+ laser and was detected by either a cooled North-Coast EO-817S Ge detector or an EG&G 250 uv Si photodiode. Changes in the luminescence intensity due to on-off modulation of the microwave power (~30 mW from a Gunn diode) or magnetic-field modulation (~1 mT at 1.2 kHz) were detected synchronously by a lock-in amplifier. All measurements were made in the Faraday geometry. A 0.25-m monochromator (Jarrel-Ash Mark X) was used for both luminescence and spectral dependence measurements.

The sample used in this study was a liquid-encapsulated Czochralski (LEC) -grown single crystal of GaP and was supplied by K. M. Lee. Oxygen incorporation in the sample was provided from boric oxide dissolved into the melt. The sample dimensions were 1 mm × 1 mm × 1.5 mm.

III. EXPERIMENTAL RESULTS

A. Luminescence study

The luminescence spectrum of the GaP:O sample at $T=1.7$ K is shown in Fig. 1(a). Despite the poor resolution, the two luminescence bands are clearly those first observed by Dean and co-workers and attributed to the oxygen defect.[2,3] The broad band with a peak at 985 nm (~1.3 eV) is the donor-acceptor transition involving the deep oxygen donor and an unknown shallow acceptor while the more structured band is due to electron capture at the oxygen defect.

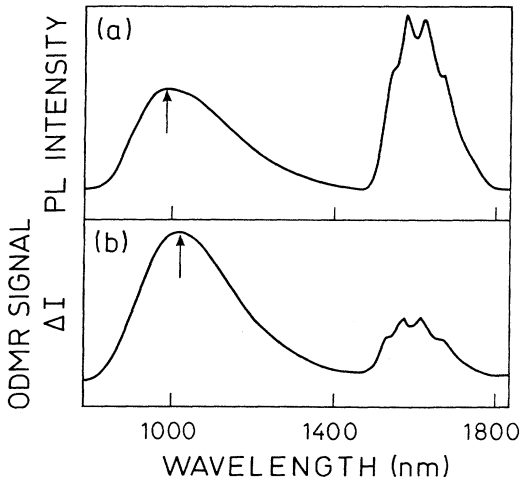

FIG. 1. (a) The near-infrared luminescence spectrum obtained from the GaP:O sample using Ar^+ laser excitation at 514.5 nm and $T=1.7$ K. (b) The spectral dependence of the $S=1$ ODMR resonance at $T=1.7$ K. The arrows in the figure show the difference in the peak position of the oxygen donor-acceptor luminescence band and the higher-energy transition of the spectral dependence spectrum.

B. ODMR spectra

Figure 2 shows the observed ODMR spectrum at 35 GHz while monitoring the total near infrared luminescence from 1000 to 1800 nm with $\mathbf{B}\|[100]$, $\mathbf{B}\|[111]$, and $\mathbf{B}\|[011]$. There are two distinct ODMR spectra in Fig. 2. The first is an isotropic quenching (the luminescence intensity decreases at resonance) transition at $B=1.24$ T which has been the subject of a recent ODENDOR study by our group.[14] It was shown that the defect is a donor situated on the P sublattice. The second spectrum in Fig. 2 with which we are concerned here is due to an anisotropic spin triplet showing resolved quartet hyperfine structure as was first reported by Gal, Cavenett, and Smith.[7] The four lines in both the high- and low-field branches of the ODMR spectrum are not equally intense, the extreme lines being broader and showing a barely resolved structure. This is as expected for a magnetic ion which has two reasonably abundant $I=\frac{3}{2}$ isotopes with slightly differing magnetic moments. A number of examples exist in the Periodic Table: Cl, Cu, and Ga, and, as pointed out by Gal *et al.*,[7] a line-shape fit would appear to indicate that Ga is the magnetic ion. In Fig. 2 we have used the same gain for each of the three ODMR spectra. The intensity of the ODMR signal drops rapidly as the sample is rotated from the [011] direction to the [100] direction. In the case of ODMR measurements of $S=1$ systems the observation of magnetic resonance is made possible because of the difference in radiative rates for the $M=0$ and ±1 levels. When the magnetic field is parallel to a defect axis the eigenvalue $M=0$ is a good quantum number and the ODMR intensity is a maximum. Rotating the sample, however, causes a mixing of the three states by off-diagonal terms and thereby a reduction in the ODMR intensity. In Figs. 3 and 4 we show the angular variation of the triplet ODMR spectrum in the $(0\bar{1}1)$ and (100) planes, respectively. The circles are the experimental points whose sizes are in proportion to the intensity of the ODMR signal. We observe that there is a large reduction in the ODMR intensity in both planes as the sample is rotated away from the [011] direction.

We find that the positions of the magnetic-resonance transitions of Figs. 3 and 4 can be fit to a C_{2v} spin Hamiltonian with the principal axis system for one of the equivalent orientations of the defect shown in Fig. 5:

$$\mathcal{H}=\mu_B\mathbf{B}\cdot\tilde{\mathbf{g}}\cdot\mathbf{S}+\mathbf{S}\cdot\tilde{\mathbf{D}}\cdot\mathbf{S}+\mathbf{I}\cdot\tilde{\mathbf{A}}\cdot\mathbf{S}\ , \tag{1}$$

where $\tilde{\mathbf{D}}$ is the fine-structure tensor and $\tilde{\mathbf{A}}$ the hyperfine tensor with either of two $I=\frac{3}{2}$ nuclei. Returning to Fig. 2(a) for a moment we see that there are a number of weak lines in the region between the strong ODMR transitions.

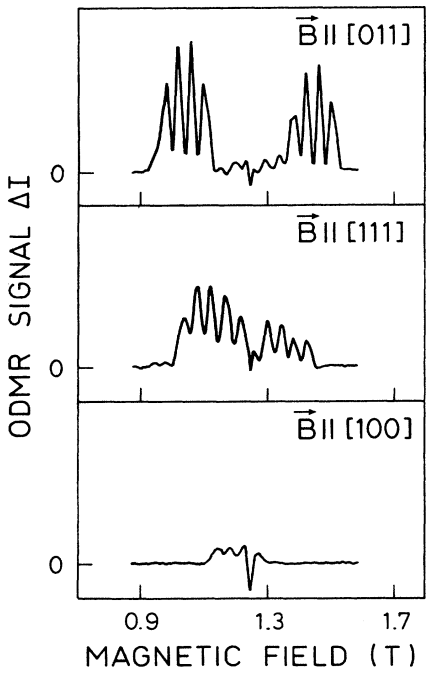

FIG. 2. The ODMR spectrum from GaP:O with $\mathbf{B}\|[011]$, [111], and [100] at $\nu_0=34.8$ GHz and $T=1.7$ K. The scale on the y axis of the three ODMR spectra is the same, showing the large reduction in the ODMR intensity from the [011] direction to the [100] direction.

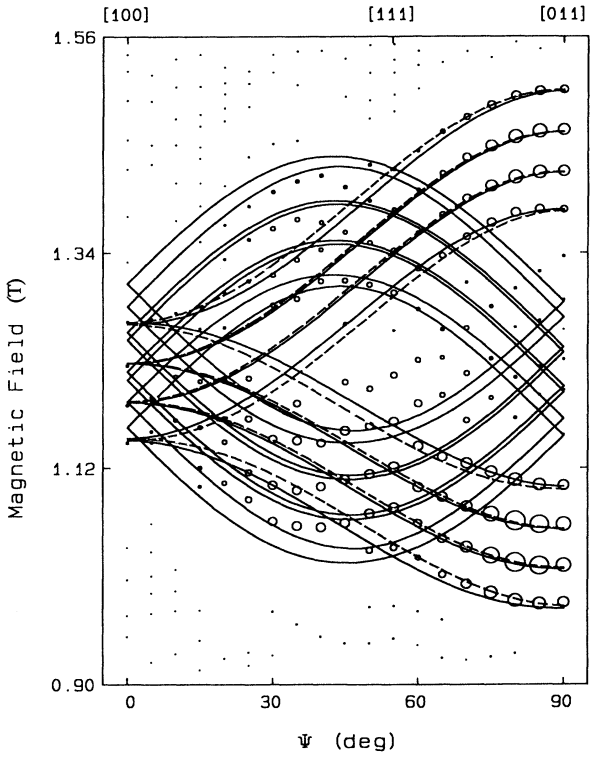

FIG. 3. The angular dependence of the ODMR, $\mathbf{B}\perp[0\bar{1}1]$. The circles are the experimental points whose size is proportional to the intensity of the ODMR transition and the lines are a theoretical fit to Eq. (1). The dashed lines show the orientation of the defect with principal axes depicted in Fig. 5, $\mathbf{B}\perp\hat{2}$.

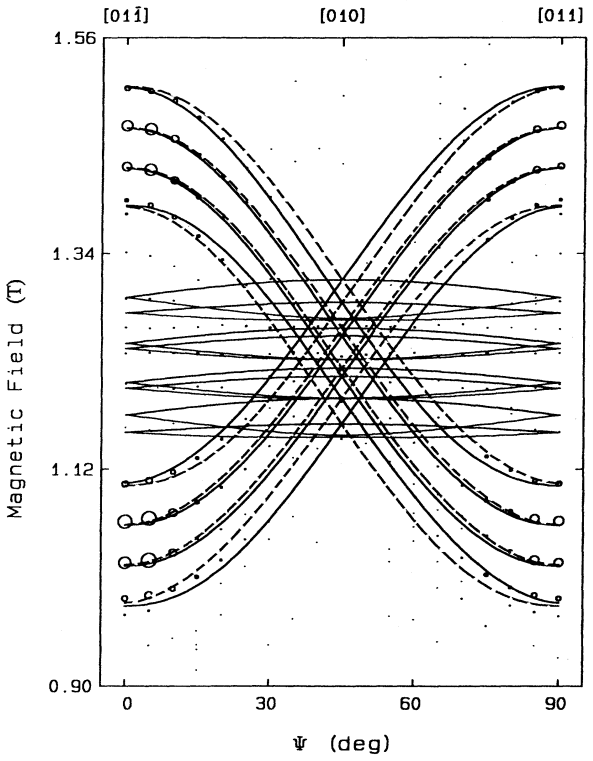

FIG. 4. The angular dependence of the ODMR, B⊥[100]. The circles are the experimental points whose size is proportional to the intensity of the ODMR transitions and the lines are a theoretical fit to Eq. (1). The dashed lines show the orientation of the defect with principal axes depicted in Fig. 5.

These lines are due to other orientations of the defect and are observed in this study for the first time. The fit to the experimental data is shown as the solid lines in Figs. 3 and 4 with the spin Hamiltonian parameters as listed in

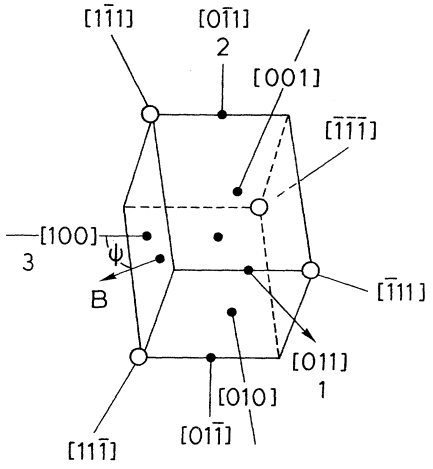

FIG. 5. The principal axes of the $\tilde{\mathbf{g}}$, $\tilde{\mathbf{D}}$, $\tilde{\mathbf{A}}$, and $\tilde{\mathbf{Q}}$ tensors used in our analysis.

TABLE I. Spin Hamiltonian parameters for the Ga-related $S=1$ defect in GaP (see Fig. 5 for the defect principal axes). The principal values of D, A, and Q are given in units of 10^{-4} cm^{-1}, and the estimated error in the last digits of each are indicated in the parentheses.

Principal axis	1	2	3
$\tilde{\mathbf{g}}$	2.000(3)	2.000(20)	2.045(10)
$\tilde{\mathbf{D}}$	+1264(30)	−1218(40)	−47(40)
$\tilde{\mathbf{A}}$ ^{69}Ga	+370(7)	+373(15)	+368(15)
^{71}Ga	+470(10)	+474(20)	+467(20)
$\tilde{\mathbf{Q}}$ ^{69}Ga	−0.87(10)		
^{71}Ga	−0.55(6)		

Table I. (In the table, the hyperfine parameters are identified with the ^{69}Ga and ^{71}Ga nuclei, which will be established unambiguously later from the ODENDOR analysis. For convenience in the presentation, therefore, we will adopt this labeling at the outset.) The dashed lines in these figures arise from the defect orientation illustrated in Fig. 5. Some of these parameters were extracted from the ODMR measurements, others from the ODENDOR measurements to be described. The fit to the data is good. We have shown the fit only for the more abundant ^{69}Ga isotope with the lower magnetic moment, the fit for the other isotope being equally good.

The spectral dependence of the triplet ODMR spectrum with B‖[011] is shown in Fig. 1(b). The disparity between the peak positions of the lower-wavelength broadbands in Fig. 1(a) and Fig. 1(b) and their relative intensities compared to the structured electron-capture luminescence is evident as has been previously pointed out by Lee[9] and by Godlewski and Monemar.[10] As pointed out by these workers, this may serve to challenge any simple connection to the oxygen-related luminescence.

C. Level crossing experiment

Using magnetic-field modulation and monitoring the luminescence intensity as a function of the magnetic field with B‖[011], we have determined the position of the level crossings of the Zeeman states of the triplet. The resulting spectrum which is derivative in nature is shown in the center of Fig. 6. The broad feature is similar to that reported by Gal *et al.*, but in addition, sharper structure at $B=0.25$ T is also observed. The spectrum remains even when the microwaves are switched off and the structure at 0.25 T is sharpest along the [011] direction demonstrating a direct relationship with the triplet $S=1$ system found in the ODMR experiment. Solving Eq. (1) by direct matrix diagonalization, the energy levels for the ^{69}Ga and ^{71}Ga isotopes were obtained and are shown in the lower and upper parts of Fig. 6, respectively, for **B** parallel to the defect $\hat{1}$ axis. The calculated true level crossing positions are indicated by continuous and dashed lines for the ^{69}Ga and ^{71}Ga isotopes, respectively.

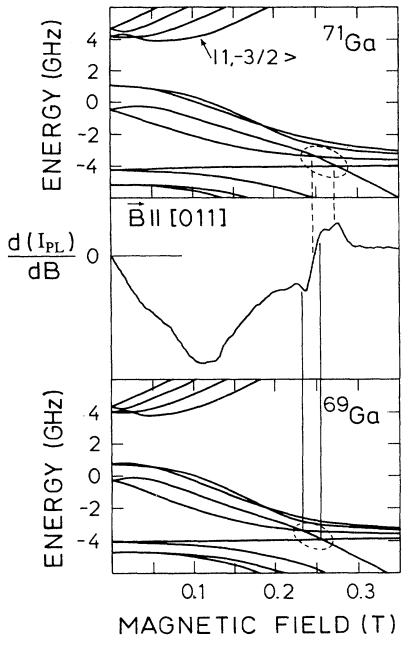

FIG. 6. The level crossing observed monitoring luminescence in the (0.6–1.1)-μm range with $\mathbf{B}\|[011]$. The energy-level scheme for the $S=1$, $I=\frac{3}{2}$ system is shown in the upper part (for ^{69}Ga) and the lower part (for ^{69}Ga). The level crossings are indicated by dashed lines (for ^{71}Ga) and solid lines (for ^{69}Ga).

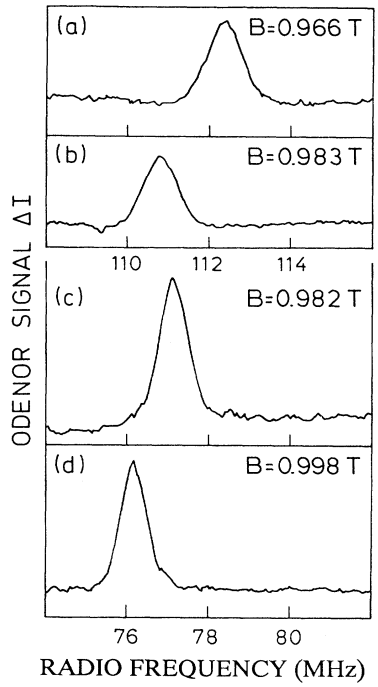

FIG. 7. The ODENDOR transitions for the lowest-field hyperfine component of the ODMR transition of Fig. 2(a). Spectra (a) and (b) are from the ^{71}Ga nucleus while (c) and (d) are from the ^{69}Ga nucleus.

The agreement between theory and experiment is very good. The broad feature at lower field in Fig. 6 is probably due to the B-dependent mixing or the other levels of this defect orientation (anticrossings) as well as those from the other defect orientations. From the analysis of Eq. (1) it was determined that A_1 has the same sign as D_1. The level ordering shown in Fig. 6 is for positive D_1 (and A_1). This is consistent with an earlier assignment for D by Gal *et al.*[7] on the basis of circular polarization detected in the ODMR. We accept this value (even though our attempts to detect consistent circular polarization results were inconclusive) because it leads to positive values of A as required for the positive Ga nuclear moments and isotropic (s function) hyperfine interactions. These signs are included in Table I.

D. ODENDOR spectra

Figure 7 shows ODENDOR spectra obtained by tuning the magnetic field to the extreme low-field ODMR transitions of Fig. 2, $\mathbf{B}\|[011]$. With $B=0.966$ T (the peak position of the partially resolved lower-field weaker ^{71}Ga hyperfine component), a single strong ODENDOR transition is observed at 112.4 MHz, as shown in Fig. 7(a). At $B=0.982$ T (the peak position of the partially resolved higher-field strong ^{69}Ga component), a single transition is observed at 77.1 MHz, as shown in Fig. 7(c).

In order to estimate the nuclear gyromagnetic ratios μ_i/I_i, we retuned the microwave frequency and again found the position of the peaks in the ODMR resonance. The new ODENDOR resonances observed are shown in Figs. 7(b) and 7(d), respectively. Assuming that dv/dB gives us the nuclear gyromagnetic ratio for the nucleus of Figs. 7(a) and 7(b) we find its value is -96.9 MHz/T while that of Figs. 7(c) and 7(d) is -57.6 MHz/T. These values are extremely large and do not correspond to the known gyromagnetic values of any known nuclear isotope. [We note, nevertheless, that the ratio of the widths of the ODENDOR line in Fig. 7(a) to that in Fig. 7(c) (1.28) is very close to the ratio of the gyromagnetic values of the two gallium isotopes, $1.27=\gamma(^{71}\text{Ga})/\gamma(^{69}\text{Ga})$.]

ODENDOR measurements were then carried out at the center of each hyperfine line with $\mathbf{B}\|[011]$ at a fixed microwave frequency. In the upper part of Fig. 8 we show the ODMR spectrum with $\mathbf{B}\|[011]$ and the results of these experiments are shown in the lower half of Fig. 8, the full and open points, whose significance we will come to later, representing the ODENDOR line positions. The number of ODENDOR lines observed depends upon which hyperfine line is being observed in the ODMR and again the frequency of each decreases with increasing B but now with slopes that differ amongst themselves and which depend also upon B.

A further set of experiments was performed in which the magnetic field was retuned a small amount within the width of a single hyperfine component. Setting the spectrometer to the peak of the hyperfine line at $B=0.982$ T the ODENDOR line position was again found to be

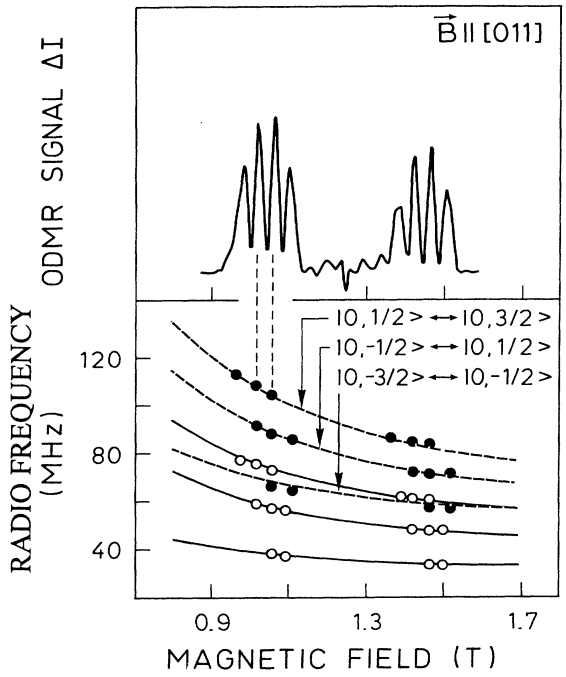

FIG. 8. The magnetic-field dependence of the ODENDOR transitions taken at a single microwave frequency. The ODMR spectrum is shown in the upper part of the diagram to indicate the position in the ODMR spectrum where the ODENDOR transitions were measured.

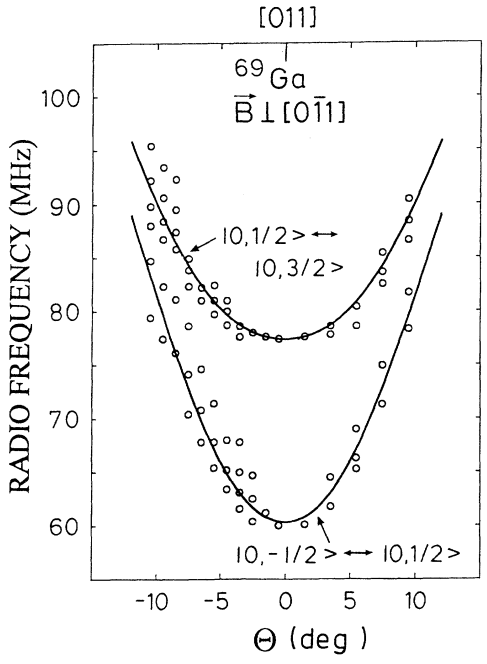

FIG. 9. ODENDOR transitions for ^{69}Ga vs the angle (θ) between **B** and the [011] direction, with **B**⊥[0$\bar{1}$1]. The open circles are the experimental frequencies observed for the $B=1.022$ T ODMR line. The solid lines are a fit to the spin Hamiltonian, Eqs. (1) and (2).

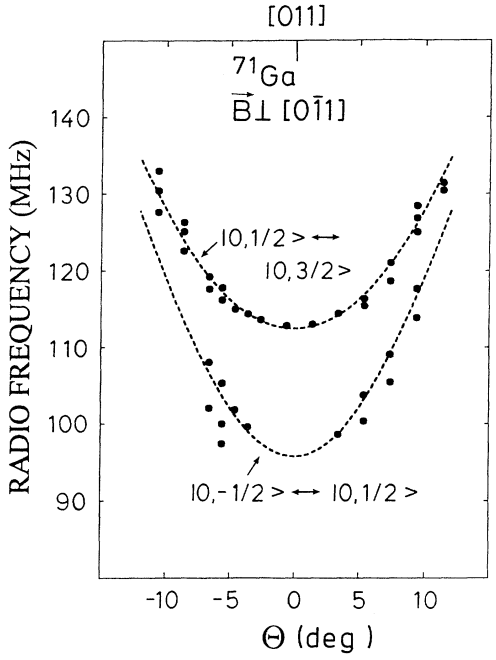

FIG. 10. ODENDOR transitions for ^{71}Ga vs θ, as in Fig. 9.

$\nu=77.10$ MHz. Retuning the magnetic field to $B=0.994$ T but keeping the microwave frequency constant we find $\nu=77.00$ MHz indicating a gyromagnetic ratio ~ -10 MHz/T. If we compare this result to those derived from Figs. 7 and 8 we see that there is a large

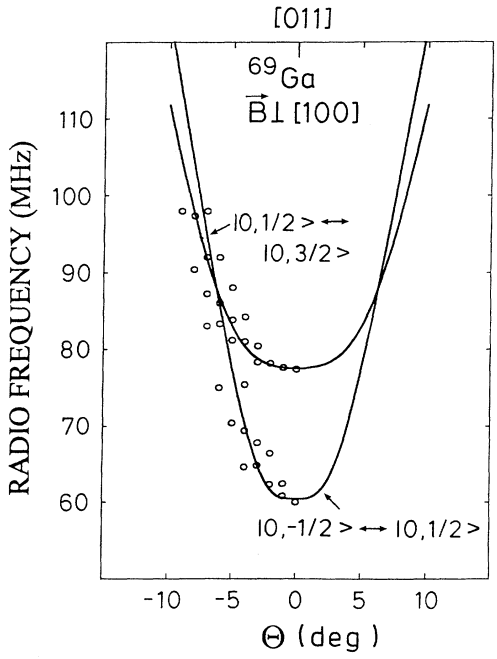

FIG. 11. ODENDOR transitions for ^{69}Ga vs θ as in Fig. 9, but with **B**⊥[100].

discrepancy in the gyromagnetic ratios calculated while in a simple picture they should have the same value in all three measurements.

The angular variation of several of the ODENDOR lines of the next-to-lowest-field hyperfine line ($B=1.022$ T) are shown in Figs. 9 and 10 for **B** in the $(0\bar{1}1)$ plane, and for the lower frequency set of ODENDOR lines in Fig. 11 with **B** in the (100) plane. All of the ODENDOR lines show a very large angular variation and split into several components as the sample is rotated away by θ from the [011] direction. The lines decreased in intensity versus θ and it was only possible to follow the spectrum $\pm 10°$ from the [011] direction.

Despite considerable experimental efforts no ODENDOR lines due to other nuclei were observed.

IV. ANALYSIS AND RESULTS

In Sec. IV B, to follow, we will analyze the ENDOR data by matrix diagonalization, the most accurate way. However, in such calculations, the simple physics is often lost. Let us therefore consider first a perturbation treatment. This will serve to establish immediately in which M state the ENDOR transitions are occurring. At the same time, the origin of the unusual field and angular dependences will become clear.

A. Perturbation analysis

Expanding the Hamiltonian of Eq. (1) to include a nuclear quadrupole interaction

$$\mathcal{H}_q=\mathbf{I}_i\cdot\tilde{\mathbf{Q}}_i\cdot\mathbf{I}_i\ , \tag{2}$$

the ODENDOR frequencies become, to first order in $Q_i/(\mu_i/I_i)B$ and second order in $A_i/g\mu_B B$ and $D/g\mu_B B$, with $\mathbf{B}\|$ to the defect $\hat{1}$ axis,

$$h\nu(M, m_i\rightleftarrows m_i-1)=|A_iM-(\mu_i/I_i)B+(3/2)Q_1(2m_i-1)-(A_i^2/2g\mu_B B)[S(S+1)-M^2+(2m_i-1)M]|\ . \tag{3}$$

Here, for simplicity, we have assumed $\tilde{\mathbf{g}}$ and $\tilde{\mathbf{A}}_i$ to be isotropic, and $\tilde{\mathbf{Q}}_i$ to have the same C_{2v} principle axes as given in Fig. 5. At this point nucleus i could be the central nucleus ($A\sim 1400$ MHz) or any other nucleus nearby.

If the ENDOR transitions being observed (40–120 MHz) were arising from either of the $M=\pm 1$ states, A_i would be only ~ 100 MHz and would necessarily arise from some nearby nucleus, unresolved in the ODMR. In this case, however, $A_i^2/g\mu_B B\sim 0.5$ MHz and the first-order terms would be sufficient. The shift versus B should give μ_i/I_i. The resonance must arise therefore instead from the $M=0$ state and the second-order term $A_i^2/g\mu_B B$ must be ~ 100 MHz, implying $A_i\sim 10^3$ MHz. We can conclude therefore that the ENDOR transitions are those for the central nucleus, the $2I=3$ transitions for each central $I=\frac{3}{2}$ nucleus accounting for the two sets of three lines of Fig. 8. The origin of the unusual field dependence is apparent now from Eq. (3), for which

$$\frac{d(h\nu)}{dB}\cong\mu/I-A^2/g\mu_B B^2\ , \tag{4}$$

which actually matches the data of Fig. 8 remarkably well, using the parameters of Table I. (The theoretical curves shown in Fig. 8 result from matrix diagonalization to be described in the next section.) The dominant large-field dependence comes from the change in the second-order hyperfine term.

[The reduced slope (~ -10 MHz/T) when the field change is within the inhomogeneous lowest-field hyperfine component can also be understood qualitatively from Eq. (3). Within a line that is inhomogeneously broadened by hyperfine fields from neighboring nuclei, B in the second-order hyperfine term of Eq. (3) can be considered the *local* field seen by a spin packet resonant at the ODMR microwave frequency which changes little as the external field sweeps through the inhomogeneous line. Viewed this way, departures from μ/I for the field dependence come only from third- and higher-order effects. A detailed development of this is beyond the scope of this paper. The phenomenon has been explored by other authors in our laboratory in considerable detail both experimentally and theoretically on a different but similar system and will be the subject of a separate publication.[15]]

Next, we consider the angular dependence. To understand its origin, it is sufficient again to consider an isotropic A and to simplify further to an axial fine structure ($D_1=D_\|$) and with $Q=0$. A nuclear spin Hamiltonian to first order in $A/g\mu_B B$ can then be written:[16]

$$\mathcal{H}_n=[A\langle S_z\rangle-(\mu/I)B]I_z+A\langle S_x\rangle I_x+A\langle S_y\rangle I_y\ . \tag{5}$$

With **B** parallel to the $\hat{1}$ axis, $\langle S_x\rangle=\langle S_y\rangle=0$, $\langle S_z\rangle=M$, which leads to the first-order terms in Eq. (3). However, as the 1-direction is rotated by θ away from $\mathbf{B}\|\hat{z}$ (in the xz plane), mixing of the M states occurs producing[16]

$$\langle S_x\rangle\cong\frac{9D_\|\sin 2\theta}{4g\mu_B B}[M^2-\tfrac{1}{3}S(S+1)]. \tag{6}$$

For the $M=0$ state, with $S=1$, this gives

$$\mathcal{H}_n(M=0)\cong-(\mu/I)BI_z-\frac{3AD_\|\sin 2\theta}{2g\mu_B B}I_x \tag{7}$$

and

$$h\nu(0, m\rightleftarrows m-1)\cong\left[[(\mu/I)B]^2+\left[\frac{3AD_\|\sin 2\theta}{2g\mu_B B}\right]^2\right]^{1/2}\ . \tag{8}$$

In our case $3AD_\|/2g\mu_B B\sim 12(\mu/I)B$, and the second term produces a rapid shift to higher frequencies for

$|\theta| > 0$, as observed. [This treatment, accurate only to first order in $A/g\mu_B B$ has not included the large second-order shifts for $\theta=0$. A more detailed treatment[15] confirms that the form of Eq. (8) is the same but with the $(\mu/I)B$ term simply replaced by $h\nu$ at $\theta=0$.]

The general features of the ENDOR spectra are therefore understood. The transitions arise from two central $I=\frac{3}{2}$ nuclei in the electronic $M=0$ state. The close match of Eq. (4) to Fig. 8 is sufficient to unambiguously identify the central nuclei as ^{69}Ga and ^{71}Ga. The unusual field and orientation effects arise from second and higher order effects due to the mixing of $M=\pm1$ states into the $M=0$ states via the large A and D terms.

B. Matrix diagonalization

The perturbation analysis of the preceding section gives an intuitive feeling for the observed experimental results. However, to obtain an accurate analysis while properly including anisotropy in $\tilde{\mathbf{g}}$, $\tilde{\mathbf{D}}$, and $\tilde{\mathbf{A}}$, and the quadrupole interaction, we have found it more convenient to use matrix diagonalization. The ODENDOR transition frequencies were solved for $\mathbf{B}\|\hat{1}$ as a function of magnetic field for the $|\pm1\rangle$ and $|0\rangle$ states. Consistent with the arguments of the preceding section, the transition frequencies obtained were found to be consistent only with ODENDOR transitions within the $|0\rangle$ state. With $\mu/I=10.23$ MHz/T for ^{69}Ga, the values $A_\perp=(A_2+A_3)/2$ and Q_1 were adjusted to obtain the best possible fit which is shown as the solid lines in Fig. 8. Using only the ratio of the nuclear gyromagnetic values and the quadrupole moments of the two gallium nuclei we found the ODENDOR transitions indicated by the dashed lines in Fig. 8. We see that the fit to all of the experimental points is very good. This analysis allowed a precise determination of the perpendicular components of $\tilde{\mathbf{A}}$ and the sign and magnitude of the quadrupole component Q_1 for the two isotopes and the results are shown in Table I. These ODENDOR transition frequencies could not be fit using the nuclear gyromagnetic values and quadrupole moments of the Cl or Cu isotopes.

The angular variation of the ODENDOR lines in Figs. 9–11 was also computed by matrix diagonalization. The results are shown as the solid lines in Figs. 9 and 11 and the dashed lines in Fig. 10. Our C_{2v} Hamiltonian, Eqs. (1) and (2), with the parameters of Table I, predicts a single line versus θ. On the other hand, the observed ODENDOR lines split into several closely spaced lines. In our fit we have therefore matched to the center of gravity of the lines. The significantly different dependence in the $(0\bar{1}1)$ and (100) planes provided a sensitive determination of D_2 and D_3. These values are included in Table I and were used in the ODMR fits of Figs. 3 and 4.

The complex splittings of the ENDOR lines versus θ suggest that the true symmetry of the defect may actually be lower than C_{2v}. Simple symmetry arguments, however, predict that this should produce at most a splitting into two ODENDOR lines versus θ with $\mathbf{B}\perp[0\bar{1}1]$ for the defect orientation shown in Fig. 5. If, at the same time, we are observing ODENDOR transitions for the $\hat{2}\perp[0\bar{1}1]$ defect as well (note the superposition of the two ODMR transitions for $\mathbf{B}\|[011]$ in Figs. 3 and 4), this could double the number to 4. It would be highly coincidental, however, if the ODENDOR spectra for both $\mathbf{B}\|\hat{2}$ and $\mathbf{B}\|\hat{1}$ superposed. We have not attempted to explore this further. We may note that since the angular dependence comes primarily from the $\tilde{\mathbf{D}}$ term, a tilt of the D_1 axis by $\sim2°$ from the [011] direction would be sufficient to produce splitting of this amount. Such a small tilt would be difficult to resolve in our ODMR spectra.

(It is interesting to note, however, that Dawei and Cavenett[8] concluded from their ODMR results that a 6° tilt existed of the D axis from the [011]. The actual principal axes they deduced and the value they estimated for $E=D_2-D_3$ differ substantially from the results of our more comprehensive ODMR and ODENDOR study, pointing out the difficulty of the analysis from the limited angular-dependence data available from the ODMR alone. Still it is interesting that they came to the conclusion of lower symmetry, a result that we have not been able to justify from analysis of our ODMR spectra alone.)

Another possible origin of the ENDOR line splitting could be the existence in the crystal of small angle grain boundaries separating domains of slightly different crystalline orientations. Since we had only one sample we could not test this. Although we consider this a less likely explanation, we cannot rule it out.

V. DISCUSSION

A. Identification of the defect

As indicated in the introduction, the identification of the defect giving rise to the ODMR spectrum of Fig. 2 has been the subject of much controversy. In this section, let us summarize what we have learned in the present study that may shed light on the identification.

First, we interpret our results to indicate that a gallium interstitial (Ga_i) is in the core of the defect, as first proposed by Lee[9] and Godlewski and Monemar.[10] The evidence is summarized below.

(i) Our ODENDOR results confirm unambiguously that the two-component $I=\frac{3}{2}$ hyperfine interaction evident in the ODMR spectrum arises from the two isotopes of a single gallium nucleus (^{69}Ga,^{71}Ga) in the core of the defect.

(ii) The magnetic hyperfine interaction is almost isotropic and large, being $\sim16\%$ off the Hartree-Fock estimate for the 4s state of a free Ga^0 atom.[17] This, in turn, is almost exactly one-half of the hyperfine constant of an isotropic $S=\frac{1}{2}$ center observed via ODMR by Lee[9] in the same oxygen-doped material which he identified as isolated Ga_i^{2+}. (He was able to rule out the alternative possibility that it arises from a Ga_P antisite on the basis of theoretical prediction of p-like character for it.[18]) A reduction by a factor of 2 in the hyperfine interaction when going from a one-electron $S=\frac{1}{2}$ system to a two-electron $S=1$ system is often encountered since the two particles tend to be spatially separated in the excited excitonic state.

Next we turn to the question as to whether oxygen may also be incorporated in the defect or not. As shown in Fig. 1, the dominant band peaked at 1020 mm observed in the spectral dependence of the ODMR is clearly distinct from the slightly higher energy oxygen donor to shallow acceptor luminescence band. This observation, previously noted by Lee[9] and by Godlewski and Monemar,[10] has been challenged by Gal[11] as perhaps the result of not properly subtracting an often present nonresonant background in the ODMR spectral dependence. In our samples, the nonresonant background was negligible. This possible connection to the isolated oxygen donor therefore appears no longer to be valid. Instead, we conclude that the 1020-nm band is probably a transition directly involved with the Ga_i-related defect. Consistent with this, the level crossing of Fig. 6 was observed directly in this band as well as definite circular polarization effects at ODMR resonance. (This again conflicts with the observation of Gal *et al.*[7] as restated recently by Gal.[11]).

On the other hand, the ODMR signal is clearly being detected in the 0.841-eV electron-capture luminescence for the isolated neutral oxygen donor. However, since the 0.841-eV luminescence has been established to display full T_d symmetry,[1] as opposed to C_{2v} (or lower) for the ODMR, the mechanism must be an indirect one. Recognizing this, Gal *et al.*[4] explained this, while retaining their ODMR identification with isolated O_P^-, by a spin-dependent Auger process, the defect ending up in the excited O_P^0 emitting state. Godlewski and Monemar[10] have suggested instead an energy transfer from the 1020-nm (1.2-eV) defect luminescence to the overlapping photoionization spectrum for O_P^0 producing enhanced subsequent capture luminescence. In their model, the defect is unrelated to the oxygen donor.

Still it is important to note that this ODMR signal has so far only been reported in oxygen-doped material. We cannot rule out therefore that oxygen does indeed form an integral part of the defect. Since the major abundant ^{16}O isotope has zero magnetic moment, our ODENDOR studies are insensitive to its presence. Unfortunately, ODENDOR lines have not been detected even for the nearby Ga and P neighboring host nuclei and the clues that these often provide to the surrounding structure are also unavailable.

Interstitial gallium should be a donor and for it to be involved in an efficient *neutral* deep bound excitonic $S=1$ luminescence, we would expect it to be compensated by the negative charge(s) of a nearby acceptor (or acceptors). Since substitutional oxygen has a deep acceptor level $(-/0)$ at $E_c-0.9$ eV, as well as its donor level $(0/+)$ at approximately the same position[1,19,20] it clearly could be involved.

Two possibilities suggest themselves for the luminescence process, consistent with an s-like Ga_i paramagnetic component of the neutral $S=1$ excited state:

$$Ga_i^0 + A^0 \rightarrow Ga_i^+ + A^- + h\nu \tag{9a}$$

or

$$Ga_i^{2+} + A^{2-} \rightarrow Ga_i^{3+} + A^{3-} + h\nu\ , \tag{9b}$$

where A denotes the nearby acceptor(s).

In Eq. (9a) the $4s$ shell of Ga_i^0 would be filled and the isotropic hyperfine interaction would have to arise from its $5s$ contribution to the bound electron state. Since the observed hyperfine interaction indicates the equivalent of $\sim 32\%$ of the neutral atom $4s$ character for the electron, it appears marginal that Ga_i^0 could account for it. Ga_i^{2+} in (9b) easily accounts for the hyperfine interaction but requires three compensating negative charges.

Before pursuing this point, let us first also consider the information available from the fine-structure D and the central gallium nuclear quadrupole interaction. The fact that $D_1 \sim -D_2$, with $D_3 \sim 0$, represents a rather special and interesting case. To the extent that this reflects an effective crystalline potential at the Ga_i site, it is interesting to note that for the quadratic terms in the potential expansion

$$V_2(\mathbf{r}) = \tfrac{1}{2}\mathbf{r}\cdot\nabla\nabla V(\mathbf{r})\cdot\mathbf{r} \tag{10}$$

two equal excess charges, one each along the $[\bar{1}11]$ and $[\bar{1}\,\bar{1}\,\bar{1}]$ direction from the central Ga_i for the defect orientation of Fig. 5, would provide the proper symmetry with

$$\frac{\partial^2 V}{\partial x_1^2} = -\frac{\partial^2 V}{\partial x_2^2}\ , \qquad \frac{\partial^2 V}{\partial x_3^2} = 0\ . \tag{11}$$

The negative value for Q_1, reflecting the field gradient along the $\hat{1}$ axis, suggests that these are negative charges, again as expected for nearby acceptor compensation.

The models of Eqs. (9a) and (9b) however appear to call for an odd number of compensating charges, which argues against the obvious suggestion of Ga_i next to a pair of substitutional acceptors, possibly O_P^-. Alternatively, we must recognize that the presence of an appropriately charged acceptor in the $[\bar{1}00]$ direction could have a tendency toward the same effective potential, its presence being telegraphed to the Ga_i via its two nearest $[\bar{1}11]$ and $[\bar{1}\,\bar{1}\,\bar{1}]$ neighbors. Such effects have been observed for zinc interstitial–zinc vacancy close pairs separated along a $\langle 100\rangle$ direction in ZnSe.[21–23]

The analogy above to the $\langle 100\rangle$-separated Zn_i-V_{Zn} pairs in ZnSe presents another intriguing possible model. Could this be related to a $\langle 100\rangle$-oriented Ga_i-V_{Ga} pair that is somehow stabilized by the nearby presence of oxygen?

In this context, it is interesting to recall the model of Chadi and Chang[24] for the DX center in AlGaAs. There, the deep state for a chemical donor on the As sublattice (D_{AS}) was predicted to result from the ejection of a neighboring Ga atom into its nearest $\langle 111\rangle$-oriented interstitial position when a second electron is captured producing a negatively charged $(Ga_i V_{Ga} D_{As})^-$, complex. Is it possible that we here are observing something closely related to the corresponding configuration for O_P^-, i.e., $(Ga_i V_{Ga} O_P)^-$, but with the Ga_i-V_{Ga} component oriented along the nearest $\langle 100\rangle$ direction?

The identification of the $S=1$ ODMR signal with the triplet state of isolated O_P^- is precisely the suggestion of

Gal *et al.* in their original, now discarded, direct luminescence model[7] and in the subsequently modified spin-dependent Auger model.[4] Our conclusion that the 1.20-eV luminescence is unrelated to the DA pair band but rather is direct luminescence from the $S=1$ state does not disprove this but makes it somewhat less likely. On the other hand, the presence of a second oxygen donor

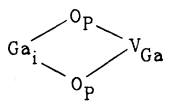

could retain C_{2v} point-group symmetry, provide an efficient, compensated, electrically neutral ($Ga_i^{2+,3+}$)-related $S=1$ luminescence center, and account for the unique $D_3 \sim 0$ fine structure. (The possible involvement of two oxygens was one of several models also considered by Dawei and Cavenett.[8])

And so it is our necessary conclusion at this stage that the direct involvement of oxygen in the core of the defect cannot be ruled out and that O_P^- related models [O_P,$(O_P)^2$, etc.] remain strong viable candidates. What our results do suggest, however, is that if O_P is involved, the local atomic arrangement involves an interstitial Ga donor, most likely compensated by a nearby $\langle 100 \rangle$-oriented gallium vacancy acceptor.

B. ODENDOR in the $M=0$ state

The detection of ODMR for an $S=1$ luminescent system is possible because the radiative lifetimes differ for the different M electronic spin states. Microwave-induced magnetic resonance transitions between these states serve therefore to transfer defects out of the "bottleneck" longer lifetime state into the more radiative ones, producing an increase in the luminescence. ODENDOR occurs when defects out of tune with magnetic resonance due to a nuclear hyperfine interaction are brought into resonance by flipping the nuclear spin, the subsequent electronic spin transition producing still additional luminescence.

In many, if not most cases, it is the $M=0$ state which is found to be the bottleneck state in photoluminescent triplet systems. This means that for ODENDOR studies, one may expect to observe primarily transitions in the bottleneck $M=0$ state. Since there is no first-order magnetic hyperfine interaction in this state, nuclei in the core of the defect with large hyperfine interaction constants will tend to be observed in the low radio-frequency region. We have demonstrated that this is the case for the ODMR $S=1$ signal studied here. The unusual effects that we have encountered here are therefore apt to be found frequently in future ODENDOR studies on such systems.

Large shifts in the ODENDOR frequencies versus B and versus orientation were found to result from coupling of the $|\pm 1\rangle$ states into the $|0\rangle$ state by the hyperfine interaction $\tilde{\mathbf{A}}$ and by the fine structure term $\tilde{\mathbf{D}}$ (with $\tilde{\mathbf{A}}$), respectively. We have outlined both a perturbative and matrix diagonalization treatment that serves to account for the behavior and to extract the relevant spin Hamiltonian parameters. This may prove useful for future workers who encounter this unusual behavior in ODENDOR.

VI. SUMMARY

Combining ODMR and ODENDOR, an improved set of spin Hamiltonian parameters for the much studied and controversial $S=1$ ODMR signal observed in the luminescence of the GaP:O have been determined. The nucleus that produces the resolved $I=\frac{3}{2}$ hyperfine structure in the ODMR spectrum has been confirmed to be gallium. Its large, almost isotropic, hyperfine interaction has been interpreted to indicate that the gallium is interstitial. Spectral dependence studies indicate that the ODMR-related band at 1.2 eV is distinct from the oxygen-donor–shallow-acceptor luminescence at ~ 1.30 V. This does not rule out, however, the possible incorporation of oxygen in the defect.

A new model has been proposed as a candidate for the defect which satisfies many of the properties of the spin Hamiltonian and of the luminescence. It is a Ga_i-V_{Ga} close pair oriented along a $\langle 100 \rangle$ axis which is stabilized by the presence of one or two substitutional oxygen donors. As such it is simply a lattice relaxed configuration of one or a pair of substitutional oxygen donors, respectively. It therefore bears a strong formal similarity to the model of Chadi and Chang[24] for the DX center in Al-Ga-As.

The ODENDOR transitions were found to arise from the $M=0$ electronic state leading to unusual field- and angular-dependent effects. Analysis to second- and third-order perturbation theory and/or matrix diagonalization was required.

ACKNOWLEDGMENTS

We would like to express our gratitude to H. J. Queisser of the Max-Planck-Institut für Festkörperforschung, Stuttgart, where some of this analysis (by J.F.D.) was performed. K. M. Lee at AT&T Bell Laboratories, Murray Hill, NJ, provided the sample used in this study. This research was carried out under the support of the National Science Foundation Grant No. DMR-85-20269.

*Present address: Physics Department, Trinity College, Dublin 2, Ireland.

[1]P. J. Dean, in *Deep Centres in Semiconductors*, edited by S. T. Pantelides (Gordon and Breach, New York, 1986), Chap. 4.

[2]P. J. Dean, C. H. Henry, and C. J. Frosch, Phys. Rev. **168**, 812 (1968).

[3]P. J. Dean and C. H. Henry, Phys. Rev. **176**, 928 (1968).

[4]M. Gal, B. C. Cavenett, and P. J. Dean, J. Phys. C **14**, 1507 (1981).

[5]R. Z. Bachrach, as described by P. J. Dean, in *Deep Centres in*

Semiconductors, Ref. 1.
[6]T. N. Morgan, Phys. Rev. B **29**, 5667 (1984).
[7]M. Gal, B. C. Cavenett, and P. Smith, Phys. Rev. Lett. **43**, 1611 (1979).
[8]Y. Dawei and B. C. Cavenett, J. Phys. C **17**, 6367 (1984).
[9]K. M. Lee, in *Defects in Electronic Materials,* edited by M. Stavola, S. J. Pearton, and G. Davies (Materials Research Society, Pittsburgh, 1988), Vol. 104, p. 151.
[10]M. Gowlewski and B. Monemar, Phys. Rev. B **37**, 2752 (1988).
[11]M. Gal, Phys. Rev. B **39**, 10 422 (1989).
[12]M. Gowlewski and B. Monemar, Phys. Rev. B **39**, 10 424 (1989).
[13]K. M. Lee, Rev. Sci. Instrum. **53**, 702 (1982).
[14]D. Y. Jeon, J. F. Donegan, and G. D. Watkins, Phys. Rev. B **39**, 3207 (1989).
[15]F. Rong, H. Sun, and G. D. Watkins (unpublished).
[16]G. D. Watkins, Phys. Rev. **155**, 802 (1967).
[17]A. K. Koh and D. J. Miller, At. Data Nucl. Data Tables **33**, 235 (1985).
[18]G. A. Baraff and M. Schluter, Phys. Rev. Lett. **55**, 1327 (1985).
[19]H. Kukimoto, C. H. Henry, and F. R. Merritt, Phys. Rev. B **7**, 2486 (1973).
[20]C. H. Henry, H. Kukimoto, G. L. Miller, and F. R. Merritt, Phys. Rev. B **7**, 2499 (1973).
[21]F. Rong and G. D. Watkins, Phys. Rev. Lett. **56**, 210 (1986).
[22]G. D. Watkins, F. Rong, W. A. Barry, and J. F. Donegan, in *Defects in Electronic Materials,* Ref. 9, p. 3.
[23]F. Rong, Ph.D. dissertation, Lehigh University, 1987. Both spectrum B and X_8 display $D_1 \cong -D_2$, $D_3 \sim 0$ and have been determined from beam-production-alignment studies to arise from Zn_i-V_{Zn} pairs aligned along the [100] $\hat{3}$ axis.
[24]D. J. Chadi and K. J. Chang, Phys. Rev. B **39**, 10 063 (1989).